Macromolecules

ARTICLE

pubs.acs.org/Macromolecules

A Facile Synthesis of Low-Band-Gap Donor−Acceptor Copolymers Based on Dithieno[3,2-*b*:2′,3′-*d*]thiophene

Sung-Yu Ku,[†,∥] Christopher D. Liman,[†,‡,∥] Daniel J. Burke,[†,§] Neil D. Treat,[†,‡,§] Justin E. Cochran,[†,§] Elizabeth Amir,[†,∥] Louis A. Perez,[†,‡] Michael L. Chabinyc,*[,†,‡,∥] and Craig J. Hawker*[,†,‡,§,∥,⊥]

[†]Materials Research Laboratory, [‡]Materials Department, [§]Department of Chemistry and Biochemistry, and [∥]Mitsubishi Chemical Center for Advanced Materials, University of California, Santa Barbara, Santa Barbara, California 93106, United States

[⊥]King Fahd University of Petroleum and Minerals, Dhahran, Saudi Arabia 31261

Supporting Information

ABSTRACT: A facile and scalable synthetic route to a soluble dithieno[3,2-*b*:2′,3′-*d*]thiophene (DTT) unit has been developed, which utilizes a Stille coupling reaction to efficiently synthesize the bisthienyl sulfide intermediate. This simplifies the overall DTT synthesis to only four steps with a 44% yield and facilitates its use as a donor unit in low-band-gap polymers. Solution processable alternating D-π−A-π polymers (DTTBTO and DTTDPP) have been synthesized with DTT as the donor unit and either a benzothiodiazole derivative (BTO) or fused ring 1,4-diketopyrrolo[3,4-*c*]pyrrole (DPP) serving as the acceptor unit. The ability to tailor the structure of these donor−acceptor systems permits a detailed understanding of structure/property relationships for band-gap engineering, absorbance, V_{oc}, and efficiency to be developed and applied to the design of high-performance organic solar cells.

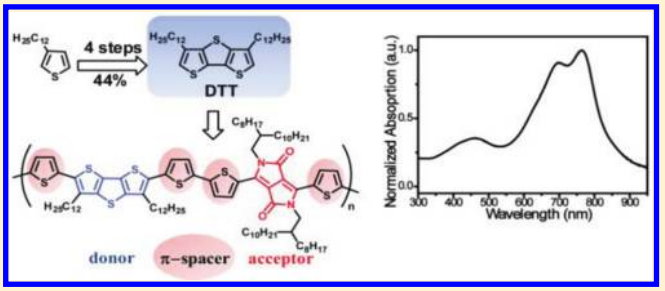

INTRODUCTION

Technologies that directly convert sunlight into electricity are attractive sources of clean, renewable energy. One of the most promising of these technologies is thin film, polymer-based organic photovoltaic devices (OPV)[1] which can be fabricated by low-cost, solution processing methods over large areas and on flexible substrates. Because of recent advances in conjugated polymer design and device fabrication techniques, the efficiencies of polymer-based photovoltaic devices are approaching 10%—the minimum often considered to make the technology commercially relevant on a large scale. These advances in photoconversion efficiency directly result from more complete absorption of the solar spectrum and a greater control of the active layer morphology.[2] One of the future challenges is to develop new p-type conjugated polymers that possess (a) sufficient solubility to enable solution processing, (b) a broad and intense absorption profile across the solar spectrum, and (c) a large free charge carrier mobility for facile charge transport.

An appropriate choice of monomers in the backbone of a semiconducting polymer can push their optical absorbance toward the near-infrared. One strategy is to incorporate electron-rich donor units and electron-deficient acceptor segments in the polymer backbone.[3] Through the "push−pull" interaction, the energy gap of the conjugated polymers decreases thus shifting the absorption band to lower energy. Another strategy is to introduce monomer units with quinoidal character into the conjugated system, which can reduce the band gap and enhance π−π stacking.[4] Fused thiophene ring systems are well-known to stabilize this quinoidal structure,[5] and alternating polymers containing fused thiophene units, such as thieno[3,4-*b*]thiophene[6] and dithieno[3,2-*b*:2′,3′-*d*]silole,[7] have achieved efficiencies of ∼7%.

Recently, oligomers that incorporate a new donor building block—the dithieno[3,2-*b*:2′,3′-*d*]thiophene (DTT) unit—have demonstrated high mobility due to the planarity and favorable sulfur−sulfur interactions for the fused DTT repeat unit.[8,9] However, the synthesis of DTT-based monomers is plagued by low yields resulting from inefficient reactions over a dozen steps. One such example is reported by He and co-workers, which utilized a ketone-based ring closure procedure for the synthesis of DTT.[9] This strategy requires double annulation reactions, which are often low yielding and unreliable. Li et al. used an alternative method to synthesize DTT based on a single ketone-based ring closure procedure.[10] However, this method requires a greater number of synthetic steps, which limits its scalability and significantly lowers the overall yield. As a result, the development of a simple and efficient method to synthesize the DTT unit is a necessity for further investigation of this promising electron-rich unit.

In this report, a reliable and scalable synthetic route to the DTT building block is demonstrated. This synthetic route utilizes a Stille coupling reaction to efficiently synthesize the bisthienyl sulfide intermediate and simplifies the overall strategy (four steps with a yield of 44%). This facilitates the use of DTT as a donor

Received: September 14, 2011
Revised: November 3, 2011
Published: November 18, 2011

Scheme 1. Possible Strategies for Preparation of the Key DTT Intermediate

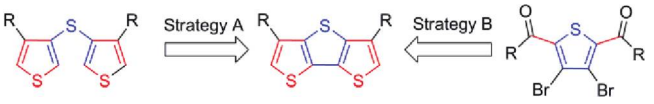

unit to construct low-band-gap polymers with two different acceptors: a benzothiodiazole derivative (BTO)[11] and the fused ring 1,4-diketopyrrolo[3,4-*c*]pyrrole (DPP).[12] A D-π−A-π alternating copolymer strategy was utilized by introducing a thiophene π-spacer between the donor and acceptor to relieve steric hindrance and achieve increased conjugation. Through this strategy, soluble, high molecular weight D-π−A-π alternating copolymers with broad, near-infrared absorption were prepared and employed in the fabrication of efficient photovoltaic devices.

RESULTS AND DISCUSSION

Material Synthesis. Previous synthetic approaches to alkyl-substituted DTT derivatives[9] have employed a double annulation approach (Scheme 1, strategy B) utilizing the diketothiophene as an intermediate. This approach suffers from numerous synthetic steps, poor yields, and an inability to scale to multigram quantities. To address this challenge, an alternative approach (strategy A) involves disconnection of the C−C thiophene−thiophene bond to give the bisthienyl sulfide intermediate, as shown in Scheme 1. Traditional strategies to form an aryl−aryl thioether bond involves quenching of aryllithium salts with sulfur electrophiles such as SCl_2 or $(PhSO_3)_2S$; however, the yields are again poor.[14] In this report, Stille cross-coupling has been utilized to synthesize the bisthienyl sulfide intermediate through a novel route, exploiting the commercially available reagent $(Bu_3Sn)_2S$, which results in quantitative generation of the desired sulfide linkage.[15]

As a result, the synthetic approach to DTT starts from commercially available 3-dodceylthiophene which on treatment with excess bromine provides the tribromo derivative **1** in 98% yield. Treatment with 2.0 equiv of *n*-butyllithium allows selective debromination to give 3-bromo-4-dodecylthiophene **2** (85% yield). The key formation of the bisthienyl sulfide intermediate, **3**, was accomplished by a double Pd-catalyzed Stille coupling reaction with $(Bu_3Sn)_2S$ and results in near-quantitative yield (98% yield). Finally, Cu-catalyzed C−C coupling reaction of **3** leads to ring closure and formation of the desired DTT building block. Through this synthetic scheme, DTT was successfully synthesized in four steps with an overall yield of 44% from commercial available 3-dodecylthiophene. This represents a significant improvement over previous strategies[9,10] and now allows multigram (10+ g) quantities of DTT to be routinely prepared.

The successful development of a facile and scalable route to DTT-based monomers now permits the exploration of this fused ring system in the synthesis of conjugated polymers, an area that has received little attention. From the limited literature, it is apparent that the main challenge for DTT-based copolymers is a relatively large energy gap, resulting in inefficient utilization of the solar spectrum. For example, an alternating D−A copolymer consisting of DTT and benzothiadiazole (BT) has a narrow absorption spectrum (absorption onset of 600 nm) that does not utilize the majority of the solar spectrum.[16] In order to broaden

Scheme 2. Synthetic Route to Functional DTT Monomer

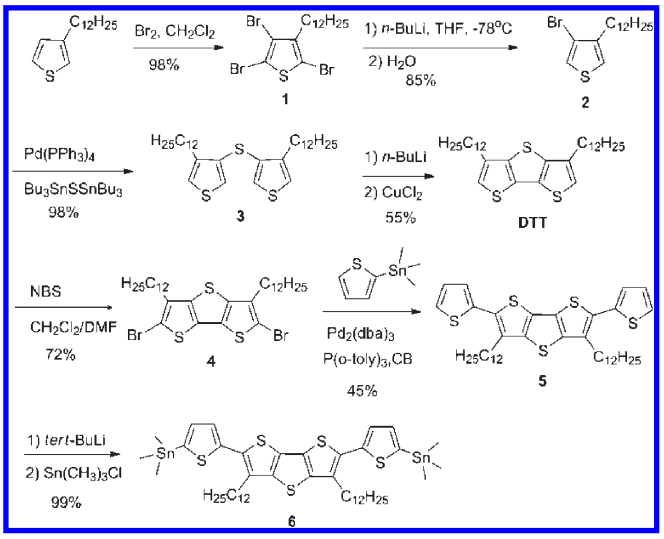

Scheme 3. Synthesis of BTO

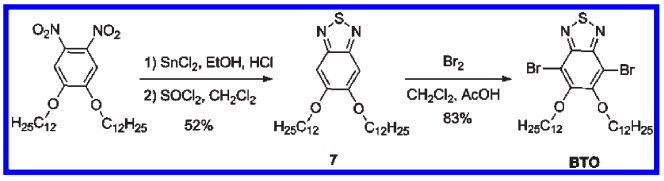

the absorption spectrum, Patil et al. reported D-π-A conjugated copolymers based on DTT and 2,3-bis((4-octyloxy)phenyl)-5,8-dithien-2-ylquinoxaline that increased the absorption edge to 700 nm through the introduction of thiophene π-spacer groups.[17] The success of this π-spacer strategy promoted the use of a similar strategy in the design of DTT monomers. To extend conjugation length with thiophene units, mild treatment of DTT with 2 equiv of NBS affords the dibromo-DTT derivatives, **4**, which is extended by Stille coupling with 2-(trimethylstannyl)thiophene to yield **5**. Finally, treatment of **5** with *tert*-butyllithium and trimethylstannyl chloride gives the bis(trimethylstannyl) monomer **6** that can now be used in Stille coupling polymerizations to obtain low-band-gap copolymers.

A benzothiodiazole derivative (BTO) and the fused ring 1,4-diketopyrrolo[3,4-*c*]pyrrole (DPP) were chosen as two different acceptors to construct low-band-gap polymers. The BTO[11] is obtained in three steps from the starting material, 1,2-dinitro-4,5-bis(dodecyloxy)benzene (Scheme 3). Reduction of the nitro groups with tin(II) dichloride gives the substituted *o*-phenylenediamine as its air-stable hydrochloride salt. Treatment with thionyl chloride affords **7**, followed by reaction with bromine to yield BTO. The DPP building block was synthesized using the literature procedure.[12]

The D-π−A-π copolymers were prepared under microwave conditions using $Pd_2(dba)_3/P(o\text{-toly})_3$ as catalyst in anhydrous chlorobenzene. Both BTO and DPP derivatives were used as acceptors, and the corresponding DTTBTO and DTTDPP D-π−A-π copolymers were obtained (Scheme 4). Significantly, all polymers showed good solubility (greater than 20 mg/mL) in chlorinated solvents, which is essential for high quality film formation using solution processing. The molecular weight and

dx.doi.org/10.1021/ma202095j |*Macromolecules* 2011, 44, 9533–9538

Scheme 4. Synthetic Routes to DTTBTO and DTTDPP Copolymers

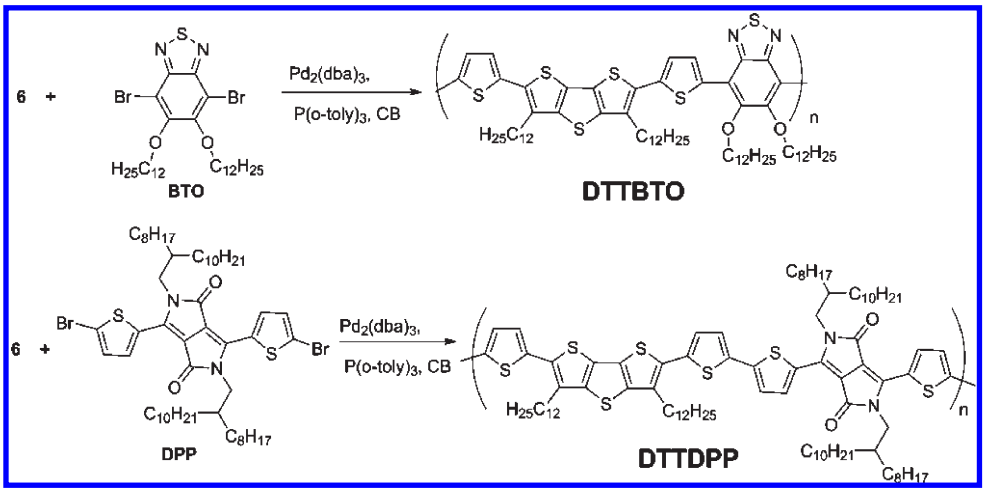

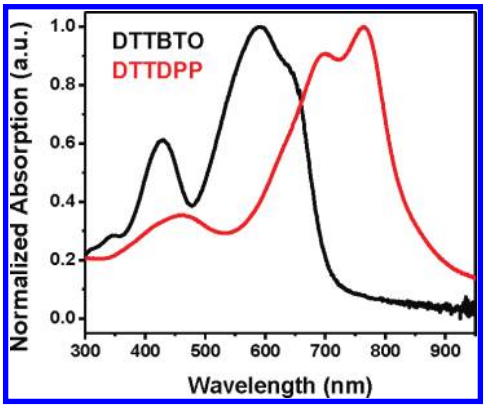

Figure 1. Thin film absorption spectra for the DTTBTO and DTTDPP D-π−A-π copolymers.

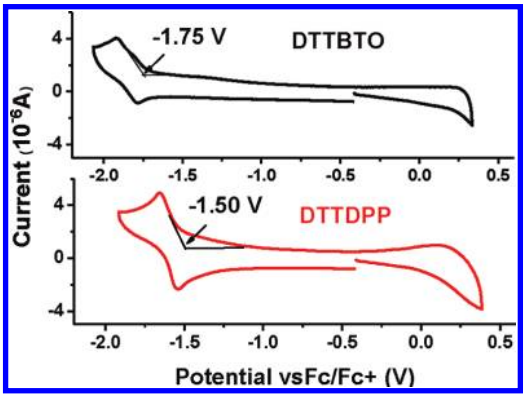

Figure 2. Cyclic voltamograms for the donor−acceptor copolymer, DTTBTO and DTTDPP. ~1 mg/mL *o*-DCB; working electrode: carbon electrode; counter electrode: Pt; reference electrode: Ag; 0.1 M nBu_4NClO_4.

polydispersity index (PDI) of the polymers were measured by GPC and calculated using polystyrene standards with DTTBTO having a number-average molecular weight, M_n, of 12 000 amu (PDI = 2.1) and DTTDPP having a significantly higher number-average molecular weight (M_n = 114 000 amu; PDI = 1.6). The increase in M_n for DTTDPP is proposed to be a result of the decreased steric interactions due to the two flanking thiophenes which have no substituents in the 3- and 4-positions when compared to DTTBTO, which has a phenyl ring with alkyloxy substituents in the 5- and 6-positions.

Physical Properties. Thin films (~55 nm) were prepared by dissolving the polymers in *o*-DCB followed by spin-coating. The absorption spectrum of the resulting thin films is reported in Figure 1 with the DTTBTO showing a broad absorption from 400 to 700 nm with maximum absorption peaks at 425 and 595 nm from the second and first excited states, respectively. The absorption onset of DTTBTO is 701 nm, and the optical band gap (E_g^{opt}) can be calculated as 1.77 eV. Significantly, substituting the DPP acceptor for the BTO acceptor to form DTTDPP resulted in a shift of the absorption edge from 700 to 891 nm and associated lowering of the optical band gap to 1.39 eV.

Electrochemical Properties. The frontier energy levels of semiconducting polymers are significant parameters for the design and modification of the polymeric repeat units in order to optimize photovoltaic devices. In this way, the energy gap between the HOMO of the p-type polymer and the LUMO of the n-type fullerene set an upper bound for the open circuit voltage (V_{oc}). The LUMO level of the p-type polymer must be offset, above that of the fullerene, to prevent charge trapping. The LUMO energy levels for the copolymers described above were obtained by cyclic voltammetry in *o*-DCB solution (Figure 2). The onset reduction potentials of DTTBTO and DTTDPP occurred at −1.75 and −1.50 V vs Fc/Fc^+, respectively, with the LUMO levels being calculated from the onset of CV reduction

Table 1. Summary of Optical and Electrochemical Properties of Polymers

	film λ^{onset} (nm)	E_g^{opt} [a] (eV)	E_{red} [b]	LUMO[c] (eV)	HOMO[d] (eV)
DTTBTO	701	1.77	−1.75	3.35 ± 0.4	5.12 ± 0.4
DTTDPP	891	1.39	−1.50	3.60 ± 0.4	4.99 ± 0.4

[a] E_g^{opt} = 1239/ λ^{onset}. [b] Potential determined by cyclic voltammetry in 0.1 M Bu_4NClO_4−*o*-DCB vs ferrocene/ferrocene$^+$. [c] LUMO = E_{red} + 5.1 (eV). [d] HOMO = LUMO + E_g^{opt}.

dx.doi.org/10.1021/ma202095j |*Macromolecules* 2011, 44, 9533–9538

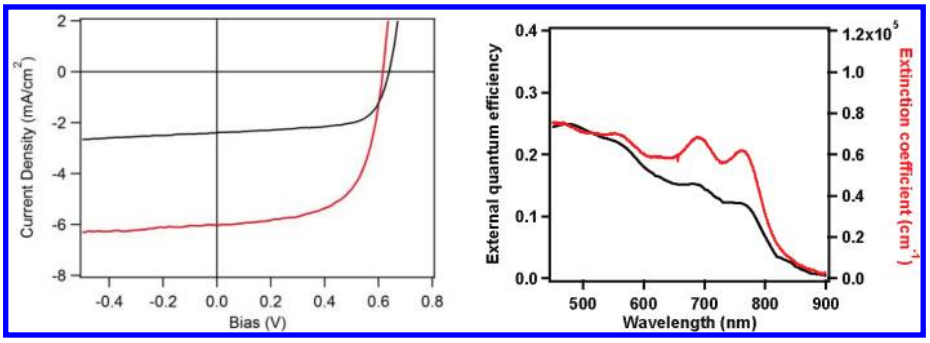

Figure 3. (a) Solar cell $J-V$ curve for DTTDPP:$PC_{71}BM$ (1:2) without additive (black) and with 9 vol % CN additive (red). (b) EQE (black) and thin film extinction coefficient (red) for DTTDPP:$PC_{71}BM$ (1:2) solar cell device with 9 vol % CN additive.

peaks using the equation LUMO = $-(E_{[\text{onset,red vs Fc}^+/\text{Fc}]} + 5.1)$ (eV).[18] This gives LUMO levels for DTTBTO and DTTDPP of 3.35 and 3.60 eV, respectively. The HOMO levels were estimated by subtracting the value for the optical band gap (determined from the absorption edge in the thin films) from the LUMO energy levels; these values have the uncertainty of the exciton binding energy, which is ~0.4 eV in many cases, and are likely underestimates.[19] The estimated HOMO values still allow relative trends in V_{oc} to be predicted. For comparison, the LUMO and estimated HOMO of P3HT are obtained by applying the same equations to the E_{red} (−2.29 V) and E_g^{opt} (1.91 eV) obtained by Janssen et al.[20] The polymers' HOMO levels (DTTDPP ~ 4.99 eV, DTTBTO ~ 5.12 eV) are ~0.3 and ~0.4 eV deeper than that of P3HT (4.72 eV),[20] respectively. The polymers' LUMO levels (DTTDPP: 3.60 eV; DTTBTO: 3.35 eV) are ~0.6 and ~0.55 eV deeper than that of P3HT (2.81 eV),[20] respectively, resulting in increased absorption without a corresponding loss in V_{oc}. A summary of the optical and electrochemical properties for the donor−acceptor copolymers is shown in Table 1.

Electrical Performance. *Thin Film Transistors.* The electrical performance of these materials was initially examined as p-type thin film transistors (TFTs). Both as-cast and annealed films of DTTBTO and DTTDPP where the annealing temperature was chosen as 150 °C based on the solvent boiling point (details of device processing and raw current−voltage data are presented in the Supporting Information) were examined. As-cast films of DTTBTO were poorly conductive, but after annealing at 150 °C for 30 min under nitrogen, improved current−voltage characteristics were observed with average saturation mobilities of 5.1×10^{-4} cm^2 V^{-1} s^{-1}, threshold voltages, V_T, of −13.0 V, and current on−off ratios, $I_{on/off}$, of 10^2. In contrast, both the as-cast and annealed films of DTTDPP showed conventional current−voltage characteristics. As-cast devices possessed average saturation mobilities of 2.8×10^{-2} cm^2 V^{-1} s^{-1}, V_T of −1.6 V, and $I_{on/off}$ of 10^3. Annealed devices showed a slight increase in average saturation mobility to 3.3×10^{-2} cm^2 V^{-1} s^{-1}, a negative shift in V_T to −4.8 V, and comparable $I_{on/off}$ of 10^3.

Photovoltaic Properties. Bulk heterojunction solar cells were fabricated using DTTDPP and DTTBTO as the donors and $PC_{71}BM$ as the acceptor. Solar cells were fabricated using DTTDPP:$PC_{71}BM$ in 1:1, 1:2, and 1:3 weight ratios with Ca/Al electrodes (fabrication details and structure are presented in the Supporting Information). The best devices that contained no additives were composed of DTTDPP:$PC_{71}BM$ (1:2), yielding an efficiency of 1.01% with a V_{oc} of 0.64 V, J_{sc} of 2.39 mA cm^{-2}, and FF of 0.67 (Figure 3a (black trace)). Significantly, the photovoltaic devices consistently had fill factors higher than

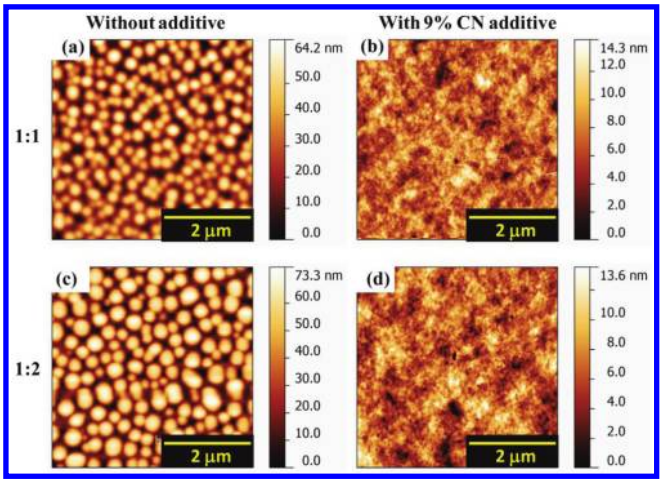

Figure 4. AFM topography images of DTTDPP:$PC_{71}BM$ (1:1) composite film (a) spin-coated from *o*-DCB solution and (b) spin-coated from *o*-DCB solution with 9 vol % CN additive. AFM topography images of DTTDPP:$PC_{71}BM$ (1:2) composite film (c) spin-coated from *o*-DCB solution and (d) spin-coated from *o*-DCB solution with 9 vol % CN additive.

Table 2. Device Parameters and Performance for DTTDPP:$PC_{71}BM$ Solar Cells

DTTDPP:$PC_{71}BM$	additive	V_{oc} (V)	J_{sc} (mA cm^{-2})	FF	PCE (%)
1:1	none	0.64	3.10	0.66	1.30
1:2	none	0.64	2.39	0.67	1.01
1:3	none	0.63	2.38	0.67	1.01
1:2	9% CN	0.61	6.09	0.63	2.35
1:2	3% DIO	0.59	5.28	0.57	1.77

other low-band-gap polymers,[6,7] suggesting efficient free charge carrier transport and collection. However, the low photocurrent for the DTTDPP:$PC_{71}BM$ device leading to lowered efficiency with the high fill factor suggests that inefficient charge generation is limiting the short-circuit current. Atomic force microscopy (AFM) analysis of the BHJs processed from *o*-DCB revealed large domains of polymer and fullerene likely leading to inefficient generation due to the relatively low interfacial area (Figure 4a,c). High boiling point additives, such as 1,8-diiodooctane (DIO) and 1-chloronaphthalene (CN), were then used to modify the polymer:fullerene phase separation and increase interfacial area.[6a,21] As expected, the active layer from the 1:1 and 1:2

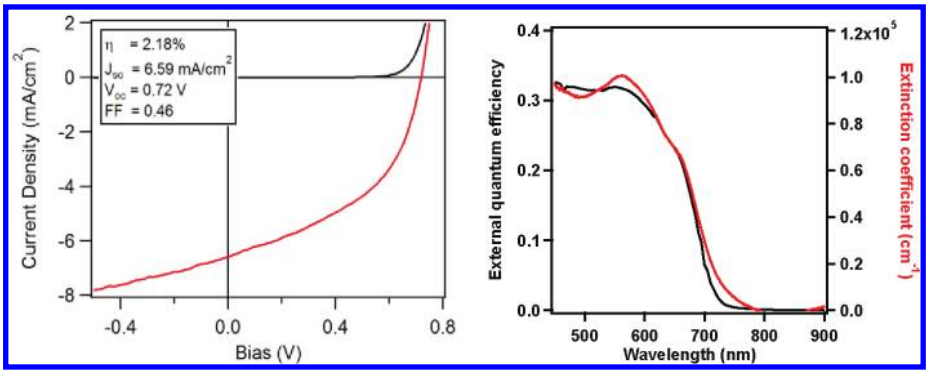

Figure 5. (a) Solar cell $J-V$ curve for DTTBTO:$PC_{71}BM$ (1:3) solar cell device with 2 vol % CN additive. (b) EQE (black) and thin film extinction coefficient (red) for DTTBTO:$PC_{71}BM$ (1:3) solar cell device with 2 vol % CN additive.

blends processed with 9 vol % CN additive in *o*-DCB show finer morphological features and increased interfacial area (Figure 4b,d), leading to an increased efficiency of 2.35% with a V_{oc} of 0.61 V, J_{sc} of 6.10 mA cm^{-2}, and FF of 0.67 (Figure 3a (red trace)). Similarly, addition of 3 vol % DIO gave finer nanoscale morphology with a corresponding improvement in J_{sc} to 5.28 mA cm^{-2} and efficiency to 1.77%.

Despite the use of additives to give nanoscale phase morphologies and more intimate mixing of polymer and fullerene domains, the J_{sc} is still relatively low in these devices. Absorption spectroscopy shows that the extinction coefficient of DTTDPP:$PC_{71}BM$ is comparable to that of P3HT:PCBM (about 5×10^4 cm^{-1}),[22] but with a wider absorption range. External quantum efficiency (EQE) measurements suggest that the relatively low J_{sc} may be due to low charge generation from photons absorbed in the DTTDPP (Figure 3b). This hypothesis is supported by the observation that at longer wavelengths (650–800 nm), where the polymer absorbs more strongly, the EQE is lower than at shorter wavelengths where the fullerene absorbance is stronger. As a result, excitons that are being generated in the polymer have a lower probability of being converted into free charge carriers which is in contrast to the behavior seen for P3HT:$PC_{61}BM$ solar cells, where it has been suggested that less efficient exciton harvesting takes place in $PC_{61}BM$ compared to P3HT, due to the smaller exciton diffusion length in the fullerene phase.[23] The behavior observed for the DTTDPP:$PC_{71}BM$ devices is similar to literature reports for other DPP-based polymers and has been attributed to a morphological effect based on solvent-induced ordering.[22] The cells studied here have higher fill factors and suggest that the origin of this behavior may be due to charge generation rather than charge extraction although further study will be required to determine the detailed mechanism of loss.

Solar cells were also fabricated using DTTBTO for comparison with the DTTDPP systems. In this case, the optimum active layer composition was a 1:3 weight ratio of DTTBTO:$PC_{71}BM$ with cells being processed using 2 vol % of CN as an additive and LiF/Al as the cathode. This device structure yielded an efficiency of 2.2% with a V_{oc} of 0.72 V, J_{sc} of 6.59 mA cm^{-2}, and FF of 0.46 (Figure 5a). The ability of the DTTBTO-based devices to give an increased V_{oc} when compared to the DTTDPP is in agreement with the deeper values for the HOMO level measured by CV. However, the lower FF (resulting from inefficient charge extraction) limited the overall device performance relative to DTTDPP. Despite the wider optical gap of DTTBTO than DTTDPP, the short-circuit current was still higher in DTTBTO due to a higher extinction coefficient and thus exciton generation in the wavelengths that it absorbs.

Table 3. Device Parameters of DTTBTO:$PC_{71}BM$ Solar Cells

DTTBTO:$PC_{71}BM$	additive	V_{oc} (V)	J_{sc} (mA cm^{-2})	FF	PCE (%)
1:2	none	0.70	3.51	0.37	0.91
1:3	none	0.69	4.11	0.37	1.06
1:3	2% CN	0.72	6.59	0.46	2.18

SUMMARY

We have developed a simple and scalable route to synthesize the fused thiophene building block, DTT, which has enabled the preparation of D-π–A-π low-band-gap copolymers with two different acceptors (BTO and DPP). The ability to tailor the structure of these materials permits design rules for these donor–acceptor systems to be demonstrated. The use of thiophene spacers allows DTTDPP to have a broader absorption spectrum (λ_{max} near 800 nm), while DTTBTO has a deeper HOMO energy level yielding a higher V_{oc}. The efficient charge transport and collection in DTTDPP devices suggests that optimization of the polymer/fullerene phase separation may lead to further increases in efficiency and to high-performance organic solar cells.

ASSOCIATED CONTENT

Supporting Information. Text giving detailed experimental procedures, characterization of all compounds, TGA, cyclic voltammetry, device fabrication and characterization, theoretical calculations, and GIWAXS data. This material is available free of charge via the Internet at http://pubs.acs.org.

AUTHOR INFORMATION

Corresponding Author

*E-mail: mchabinyc@engineering.ucsb.edu (M.L.C.); hawker@mrl.ucsb.edu (C.J.H.).

ACKNOWLEDGMENT

N.D.T. acknowledges support from the ConvEne IGERT Program (NSF-DGE 0801627) and NSF Graduate Research Fellowship. This work was partially supported by the Mitsubishi Chemical Center for Advanced Materials at UCSB. We thank the NSF SOLAR program (CHE-1035292) and NSF-DMR (DMR-0906224), funded under the American Recovery and

Reinvestment Act of 2009, for additional support of this work. Portions of this research were carried out at the SSRL, a national user facility operated by Stanford University on behalf of the U.S. Department of Energy, Office of Basic Energy Sciences, and the MRL Central Facilities which supported by the MRSEC Program of the NSF under Award DMR-1121053, a member of the NSF-funded Materials Research Facilities Network.

REFERENCES

(1) Gunes, S.; Neugebauer, H.; Sariciftci, N. S. *Chem. Rev.* **2007**, *107*, 1324.

(2) (a) van Bavel, S. S.; Barenklau, M.; With, G.; Hoppe, H.; Loos, J. *Adv. Funct. Mater.* **2010**, *20*, 1458. (b) Hoppe, H.; Sariciftci, N. S. *J. Mater. Chem.* **2006**, *16*, 45. (c) Shaheen, S. E.; Brabec, C. J.; Sariciftci, N. S. *Appl. Phys. Lett.* **2001**, *78*, 841.

(3) (a) Kitamura, C.; Tanaka, S.; Yamashita, Y. *Chem. Mater.* **1996**, *8*, 570. (b) Sahu, D.; Padhy, H.; Patra, D.; Huang, J.; Chu, C.; Lin, H. C. *J. Polym. Sci., Part A: Polym. Chem.* **2010**, *48*, 5812–5823. (c) Wu, C. S.; Chen, Y. *J. Polym. Sci., Part A: Polym. Chem.* **2010**, *48*, 5727–5736. (d) Akbaşoğlu, N.; Balan, A.; Baran, D.; Cirpan, A.; Toppare, L. *J. Polym. Sci., Part A: Polym. Chem.* **2010**, *48*, 5603–5610. (e) Hsu, S. L.; Chen, C. M.; Wei, K. H. *J. Polym. Sci., Part A: Polym. Chem.* **2010**, *48*, 5126–5134.

(4) Bredas, J. L. *J. Chem. Phys.* **1985**, *82*, 3808.

(5) (a) Wudl, F.; Kobayashi, M.; Heeger, A. J. *J. Org. Chem.* **1984**, *49*, 3382. (b) Pomerantz, M.; Chaloner-Gill, B.; Harding, L. O.; Tseng, J. J.; Pomerantz, W. J. *J. Chem. Soc., Chem. Commun.* **1992**, 1672.

(6) (a) Liang, Y.; Xu, Z.; Xia, J.; Tsai, S. T.; Wu, Y.; Li., G.; Ray, C.; Yu, L. *Adv. Mater.* **2010**, *22*, E135. (b) Hou, J.; Chen, H.-Y.; Zhang, S.; Chen, R. I.; Yang, Y.; Wu, Y.; Li, G. *J. Am. Chem. Soc.* **2009**, *131*, 15586. (c) Liang, Y.; Wu, Y.; Feng, D.; Tsai, S. T.; Li, G.; Ray, C.; Yu, L. *J. Am. Chem. Soc.* **2009**, *131*, 7792.

(7) Chu, T.-Y.; Lu, J.; Beaupre, S.; Zhang, Y.; Pouliot, J.-R.; Wakim, S.; Zhou, J.; Leclerc, M.; Li, Z.; Ding, J.; Tao, Y. *J. Am. Chem. Soc.* **2011**, *133*, 4250.

(8) (a) Okamoto, T.; Kudoh, K.; Wakamiya, A.; Yamaguchi, S. *Chem.—Eur. J.* **2007**, *13*, 548. (b) Li, X.; Sirringhaus, H.; Garnier, F.; Holmes, A. B.; Moratti, S. C.; Feeder, N.; Clegg, W.; Teat, S. J.; Friend, R. H. *J. Am. Chem. Soc.* **1998**, *120*, 2206.

(9) He, M.; Zhang, F. *J. Org. Chem.* **2007**, *72*, 442.

(10) Li, J.; Tan, H.; Chen, Z.; Goh, W.; Wong, H.; Ong, K.; Liu, W.; Li, C. M.; Ong, B. S. *Macromolecules* **2011**, *44*, 690.

(11) Helgesen, M.; Gevorgyan, S. A.; Krebs, F. C.; Janssen, R. A. J. *Chem. Mater.* **2009**, *21*, 4669.

(12) (a) Li, Y.; Singh, S. P.; Sonar, P. *Adv. Mater.* **2010**, *22*, 4862. (b) Woo, C. H.; Beaujuge, P. M.; Holcombe, T. W.; Lee, O. P.; Frechet, J. M. J. *J. Am. Chem. Soc.* **2010**, *132*, 15547.

(13) Howard, M. J.; Heirtzler, F.; Dias, S. I. G. J. *J. Org. Chem.* **2008**, *73*, 2548.

(14) Barbarella, G.; Favaretto, L.; Sotgiu, G.; Antolini, L.; Gigli, G.; Cingolani, R.; Bongini, A. *Chem. Mater.* **2001**, *13*, 4112.

(15) (a) Miguel, L. S.; Porter, W. W., III; Matzger, A. J. *Org. Lett.* **2007**, *9*, 1005. (b) Fong, H. H.; Pozdin, V. A.; Amassian, A.; Malliaras, G. G.; Smilgies, D.; He, M.; Gasper, S.; Zhang, F.; Sorensen, M. *J. Am. Chem. Soc.* **2008**, *130*, 13202.

(16) Zhang, S.; Guo, Y.; Fan, H.; Liu, Y.; Chen, H.; Yang, G.; Zhan, X.; Liu, Y.; Li, Y.; Yang, Y. *J. Polym. Sci., Part A: Polym. Chem.* **2009**, *47*, 5498.

(17) Patil, A. V.; Lee, W.; Lee, E.; Kim, K.; Kang, I.; Lee, S. *Macromolecules* **2011**, *44*, 1238.

(18) (a) Trasatti, S. *Pure Appl. Chem.* **1986**, *58*, 955. (b) Hansen, W. N.; Hansen, G. J. *Phys. Rev. A* **1987**, *36*, 1396. (c) Cardona, C. M.; Li, W.; Kaifer, A. E.; Stockdale, D.; Bazan, G. C. *Adv. Mater.* **2011**, *23*, 2367.

(19) Hwang, J.; Kim, E.-G.; Liu, J.; Bredas, J.-L.; Duggal, A.; Kahn, A. *J. Phys. Chem. C* **2007**, *111*, 1378.

(20) Veldman, D.; Meskers, S. C. J.; Janssen, R. A. J. *Adv. Funct. Mater.* **2009**, *19*, 1.

(21) Jo, J.; Gendron, D.; Najari, A.; Moon, J. S.; Cho, S.; Leclerc, M.; Heeger, A. J. *Appl. Phys. Lett.* **2010**, *97*, 203303.

(22) Zhokhavets, U.; Erb, T.; Gobsch, G.; Al-Ibrahim, M.; Ambacher, O. *Chem. Phys. Lett.* **2006**, *418*, 347.

(23) Burkhard, G. F.; Hoke, E. T.; Scully, S. R.; McGehee, M. D. *Nano Lett.* **2009**, *9*, 4037.